The genetic control of leaf and petal allometric variations in *Arabidopsis thaliana*

Xin Li
Northeast Institute of Geography and Agroecology, Chinese Academy of Sciences
Yaohua Zhang
Northeast Institute of Geography and Agroecology, Chinese Academy of Sciences
https://orcid.org/0000-0001-6360-5195
Suxin Yang (yangsuxin@iga.ac.cn)
CAS Key Laboratory of Soybean Molecular Design Breeding, Northeast Institute of Geography and Agroecology, Chinese Academy of Sciences
Chunxia Wu
Shandong Normal University College of Life Sciences
Qun Shao
Shandong Normal University College of Life Sciences
Xianzhong Feng
Northeast Institute of Geography and Agroecology Chinese Academy of Sciences

Research article

Keywords: Arabidopsis thaliana, Leaf and petal, Allometric variation, QTL mapping, Multiparent Advanced Generation Intercross Lines

Posted Date: September 13th, 2020

DOI: https://doi.org/10.21203/rs.2.20553/v2

Version of Record: A version of this preprint was published at BMC Plant Biology on December 7th, 2020.
See the published version at https://doi.org/10.1186/s12870-020-02758-w.

Abstract

Background Organ shape and size co-variation (allometry) is an essential concept for the study of evolution and development. Although ample research has been conducted on organ shape and size, little of it has considered the correlated variation of these two traits and quantitatively measured the variation in a common framework. The genetic basis of allometry variation in a single organ or among different organs is also relatively unknown.

Results A principal component analysis (PCA) of organ landmarks and outlines was conducted and used to quantitatively capture shape and size variation in leaves and petals of multiparent advanced generation intercross (MAGIC) populations of Arabidopsis thaliana . PCA indicated that size variation was a major component of allometry variation and revealed negatively correlated changes in leaf and petal size. After QTL mapping, five QTLs for the fourth leaf, 11 QTLs for the seventh leaf, and 12 QTLs for the petal size and shape were identified. These QTLs were not identical to those previously identified, with the exception of the ER locus. The allometry model was also used to measure the leaf and petal allometry covariation to investigate the evolution and genetic coordination between homologous organs. Totally, 12 QTLs were identified in association with the fourth leaf and petal allometry covariation, and eight QTLs were identified to associate with the seventh leaf and petal allometry covariation. In these QTL confidence regions, there were important genes associated with cell proliferation and expansion with alleles unique to the maximal effects accession. Besides that, the QTLs associated with life-history traits, such as days to bolting, stem length, and rosette leaf number, which was highly coordinated with climate change and local adaption, were QTL mapped and showed an overlap with leaf and petal allometry, which explained the genetic basis for their correlation.

Conclusions This study explored the genetic basis for leaf and petal allometry and their interaction, which may provide important information for investigating the organ shape and size correlated variation and evolution in Arabidopsis .

Background

The organ morphology is determined by its shape and size, and the coordinated variation in shape and size is a major component of natural diversity. Allometry refers to the size-related changes of morphological traits and could be used to describe the correlated variation in shape and size that can occur within one type of organ or can involve the relative proportions of different organs (Langlade et al., 2005; Feng et al., 2009; Klingenberg, 2016). Even closely related species can still show very different allometries, possibly due to the correlations resulting from selection (Galen, 2006; McDonald et al., 2003) and developmental constraints (Smith et al., 2014). Leaves and petals, for example, are homologous organs that share mechanisms of developmental control (Anastasiou and Lenhard, 2007; Powell and Lenhard, 2012) so that genes that act pleiotropically on both organ types might give rise to coordinating changes in shape or size. The genetic and evolutionary basis for allometric variation is integral to our understanding of plant development. However, these are poorly understood.

Addressing this question requires a quantitative genetic framework that incorporates allometric relationships, so as to allow differences intra-species to be evaluated in relation to gene action. Size differences can be expressed in terms of rather simple one-dimensional measurements (e.g. length, height etc.). Shape, on the other hand, is a much more complex feature, and it is far more difficult to measure and compare. In the 1980s, advances in the development of statistical analytic tools and their combination with outline and landmark data revolutionized the field of geometric morphometrics (Prpic and Posnien, 2016). A point and outline approach was first amplified to quantify allometric variation within the leaves of the snapdragon (Antirrhinum) species (Langlade et al., 2005). Covariation in the positions of multiple points around leaf outlines was described in terms of principal components (PCs) that captured variation in both shape and size. The principal component analysis (PCA) on the parameters then allowed the major sources of variation to be identified. This method captures allometric variation directly without making a shape and size separation, and also achieved the incorporation of different types of organ within the same framework. It was applied to quantify the allometric variation between leaves and flowers in Antirrhinum, and the resulting measures of allometry allowed underlying genes to be mapped as quantitative trait loci (QTLs) in a genetically segregating population (Feng et al., 2009; Costa et al., 2012).

Arabidopsis thaliana is an ideal organism for the study of natural variation in leaf and petal shape and size because there are extensive variations among worldwide accessions for both of these traits and for many life-history traits (Alonso-Blanco and Koornneef, 2000; Kover et al., 2009; Weigel, 2012). Leaves and petals have an advantage, as both their shapes and sizes can be readily captured for an initial approximation by a two-dimensional (2D) outline. Previous studies specifically featured a QTL analysis on leaf and petal shape and size in *Arabidopsis thaliana*. Recombinant inbred lines (RILs) from a *Ler-0* × *Col-4* cross identified a total of 16 and 13 QTL-harboring, naturally occurring alleles that contributed to natural variations in the architecture of juvenile and adult leaves, respectively (Pérez-Pérez et al., 2002). In the *Ler* × *Cvi* RIL population, eight QTLs for petal traits and three QTLs for leaf traits were identified (Juenger et al., 2005). Abraham et al. (2013) found 23 QTLs for variation in petal length, width, area, and shape in two RIL populations (*Col-0*×*Est-1* and *Ler-0*×*Col-4*). In addition, many factors controlling leaf and petal shape and size have been identified and have shown to be regulated by hormonal signals, transcription factors and miRNAs during leaf and petal development, as well as recent findings, have highlighted the contribution of mechanical signals to leaf and petal growth (Czesnick and Lenhard, 2015; Moyroud and Glover, 2017; Maugarny-Calès and Laufs, 2018). However, neither these QTLs nor the factors identified could capture the allometry variation of leaves and petals due to the limitation of the common measures in capturing the shape variation fully and in integrating the analysis of shape and size (Klingenberg, 2003).

In this study, we investigated the genetic basis of natural allometry variation in leaves and petals using a set of RILs of *Arabidopsis thaliana* that were derived from multiparent advanced generation intercross (MAGIC) lines, which were constructed by 19 founder accessions (Kover et al., 2009). Multiparent lines are better for addressing genetic correlations due to the larger number of alleles and recombination events, which allows for mapping to smaller intervals (Kover et al., 2009). In addition, the larger number

of alleles improves the ability to determine whether the distributions of allelic effects are compatible with pleiotropy. Moreover, we used a quantitative approach based on a PCA of landmark positions to define allometric spaces that captured variation in shape and size (Langlade et al., 2005; Bensmihen et al., 2008; Feng et al., 2009; Costa et al., 2012), which was treated collectively to allow allometric relationships to be defined.

Results

Allometry models of leaves and petals in MAGIC lines

To examine the allometric variation of leaves and petals within *Arabidopsis thaliana*, an allometric method based on a PCA of organ landmarks and outlines was used to quantify this trait. The Leaf4, Leaf7 and the petals from MAGIC lines were modeled and generated a data set separately (Supplementary Figure 1). And then the PCA was applied to detect the variation in the positions of points and to identify trends in shape and size variations among MAGIC lines. The resulting principal components (PCs) were ranked according to the proportions of the total variance that each of them described (Figure 1).

In Leaf4, the PCA revealed that 90.92% of the variance in organ shape and size was attributed to two PCs (Figure 1A). The Leaf4.PC1 of this model accounted for 76.84% of the total variance and affected the leaf size. Higher PC1 values corresponded to larger leaves, whereas lower values yielded smaller leaves. PC2 accounted for 14.08% of the variance and affected mainly shape. Lower values of PC2 yielded rounded leaves with a short petiole, whereas high values yielded elongated leaves with a long petiole. PC3 accounted for 3.30% of the variance and reflected the way the petiole twisted when the leaves were flattened. Its values were not significantly different between genotypes, and it was therefore excluded from further analysis.

In Leaf7, the PCA revealed that 95.25% of the variance in organ shape and size could be attributed to three PCs (Figure 1B). The Leaf7.PC1 of this model accounted for 80.27% of the total variance and affected mostly size; however, there was also a minor effect on shape. Higher PC1 values corresponded to larger, more elongated leaves, whereas lower values yielded smaller and more rounded leaves. PC2 accounted for 11.42% of the variance and mostly affected the steepness of the transition from petiole to blade, with low values yielding a very gradual transition, and high values yielding a long petiole with a steep transition. PC3 accounted for 3.56% of the variance and affected mainly the shape. Lower values of PC3 yielded more elongated and narrower leaves, whereas higher values of PC3 yielded more rounded and wider leaves.

In petals, the PCA revealed that 92.02% of the variance in organ shape and size could be attributed to two PCs (Figure 1C). The PC1 of this model accounted for 85.43% of the total variance and affected petal size. Higher PC1 values corresponded to larger petals, whereas lower values yielded smaller petals. PC2 accounted for 6.59% of the variance and affected mainly the shape. Low values of PC2 yielded elongated petals with a narrower shape, and high values of PC2 yielded rounded petals with a wider shape. PC3

accounted for 3.63% of the variance and was reflected in the petal twisting when the petals were flattened. Its values were not significantly different between genotypes, and it was therefore excluded from further analysis.

The allometric variation captured by PCs reflected both genetic differences and environmental variations within the plant growth chamber in which plants were grown. Extensive phenotypic variation was observed for all traits measured among the MAGIC lines (Table 1). An estimate of the relative genetic contribution was made by comparing the variance of each PC among MAGIC lines (which was largely due to genetic differences) to that within each line (Supplementary Figure 2). Estimates from an average of about eight plants from each of collected lines suggested that most of the variance (>60% for the PCs) had an underlying genetic basis (Table 1).

A correlation analysis between shape and size was also performed, and a number of significant pairwise correlations were observed (Figure 2). The Leaf4.PC1 was significantly positively correlated with Leaf7.PC1, which represented the leaf size. The Leaf4.PC2 was significantly correlated with Leaf7.PC2 and leaf7.PC3, which represented the leaf shape. Moreover, the leaf shape and size showed significant correlations with petals. The Petal.PC1 was significantly correlated with Leaf4.PC1 and Leaf7.PC1, which showed the negative size correlation between leaf and petal. Additionally, both the leaf4.PC2 and Leaf7.PC2 were significantly positively correlated with Petal.PC1 and negatively correlated with Petal.PC2. The correlation between the leaf and petal allometry model indicated the genetic dependency and evolution correlation in controlling leaf and petal allometry. Plus, a pairwise correlation analysis was also performed between the life history traits and the leaf and petal allometry model (Figure 2). Leaf4.PC1 was correlated with rosette leaf number and stem height; Leaf4.PC2 was highly correlated with branch number and pod number; Leaf7.PC1 was correlated with days to bolting, days to flower and stem height; Leaf7.PC2 was highly positive correlated with days to bolting, days to flower, rosette leaf number, and branch number; Petal.PC1 was correlated with rosette leaf number and branch number; and Petal.PC2 was correlated with days to bolting and days to flower.

QTLs accounted for leaf and petal allometry

To examine the genetic basis for shape and size variation of leaves and petals along the PCs in the MAGIC lines, we treated each PC as a quantitative trait, whose variation frequency showed as a normal distribution (Figure 2, Supplementary Figure 3) for QTL mapping. In the MAGIC lines QTL mapping, the PCs for leaf and petal allometry model, and 1260 SNP markers among the 19 founder ecotypes were used. We then calculated a series of QTLs associated with the variance of leaf and petal shape and size (Figure 5, Supplementary Table 2, Supplementary Figure 4, 5 and 6). In the leaf model, the QTL analysis for Leaf4.PC1 identified four QTLs located on chromosomes 1 and 3 and one QTL located on chromosome 2 for Leaf4.PC2. For the Leaf7.PC1, five QTLs were observed on chromosome 3, one QTL was located on chromosome 2 for Leaf7.PC2, and four QTLs were located on chromosomes 1 and 2 for Leaf7.PC3. In the petal model, three QTLs were identified on chromosomes 1 and 4 in Petal.PC1, and nine QTLs were identified on chromosomes 1, 2, 3, and 5 in Petal.PC2.

After comparing the position for all the QTLs identified, there was some QTL overlapping in the leaf and petal allometry model. The QTLs for PC2 of the leaf (Leaf4.PC2: LF4_2.1, Leaf7.PC2: LF7_2.1) and petal (Petal.PC2: PE_2.5) on chromosome 2 (~11 Mb) overlapped, and the alleles from the *Ler*-0 accession formed the most rounded leaves and petals with the widest shape (Supplementary Table 3). This QTL likely stemmed from the mutation of *ERECTA*, which is known to affect fruit length, and is due to the allele from the *Ler-0* accession (Abraham et al., 2013). With the exception of the ER locus for the leaf and petal shape, the QTLs LF7_1.1, LF7_1.2, LF7_1.3, LF7_1.4, and LF7_1.5 for leaf7.PC1 on chromosome 3 overlapped with QTL PE_2.6 for Petal.PC2. Moreover, the QTLs LF7_1.3, LF7_1.4, and LF7_1.5 also overlapped with QTL PE_2.7 for Petal.PC2, whereas these QTLs all showed an uncorrelated allele effect distribution (Supplementary Table 3). For the fourth and the seventh leaf, except for the overlapped ER locus (Leaf4.PC2: LF4_2.1, Leaf7.PC2: LF7_2.1) for PC2 described above, the QTLs LF4_1.3 and LF4_1.4 for leaf4.PC1 overlapped with QTL LF7_1.6 for leaf7.PC1 on chromosome 3, and showed the same allele effect distribution with a maximum value in the *Mt-0* accession and a minimum value in the *Can-0* accession (Supplementary Table 3). The overlapped QTLs might have explained the phenotype correlation and indicated the correlated genetic modules for leaf and petal allometry in evolution.

Candidate genes for leaf and petal allometry

The genes that explain natural variations in leaf and petal allometry have remained largely unknown. To identify possible candidate genes, we searched for genes containing nonsynonymous SNPs unique to accession according to PC distribution among these accession alleles (Supplementary Table 3). Based on the resequencing and reannotation of the 19 parental accessions (Gan et al., 2011), we identified candidate genes with unique allele referring to the maximal effects accession in the 95% confidence region (Supplementary Table 4). In the Leaf4 allometry model, Auxin receptor *TIR1*, Brassinolide signaling regulator *BSL3*, and *TIR1*, contributing to the flowerING time repression, had allelic variation in the coding sequence unique to the accession. In the Leaf7 allometry model, hormonal related genes, such as *SUA* (a suppressor of *abi3-5)*, *ARGOS*, serine/threonine-protein kinase *PID2*, *BRI1 suppressor 1 (BSU1)-like 3*, and *ABI4* genes, had allelic variation in the coding sequence. Moreover, the flower time regulators *ELF3* and *ELF4*, the receptor kinase *ERECTA*, cell-wall modification related genes and some transcription factors conferred allelic variations unique to the maximal effects accession.

In the petal allometry model, there were 23 genes identified with variations unique to the accession. Among these genes, the *PTL* in Petal.PC2 encodes a trihelix transcription factor whose expression is limited to the margins of floral and vegetative organs. It is involved in limiting lateral growth of organs, and recessive mutations have been found to be defective in organ initiation and orientation in the second whorl (Kaplan-Levy et al., 2014). The *OFP13* in Petal.PC2 encodes a member of the plant-specific OVATE family of proteins. Members of this family have been shown to bind to KNOX and BELL-like TALE class homeodomain proteins and function as a transcriptional repressor that suppresses cell elongation (Wang et al., 2011). The *SEU* in Petal.PC1 encodes a transcriptional co-regulator of AGAMOUS that coordinates with LEUNIG to repress AG in the outer floral whorls. Other genes, including the cell cyclin-related protein Cyclin A1;1, the protein kinase, the CYP family protein, the photoperiod-associated ELF6, and the

transcription-related genes with nonsynonymous SNPs also contribute to the petal PCs. The identified QTL and candidate genes gave us a valuable reference for insight into leaf and petal allometry.

The genetic basis for leaf and petal covariation in allometry models

Leaves and petals are homologous organs sharing mechanisms of developmental control, such that genes that act pleiotropically on both organ types might give rise to coordinating changes in shape or size. In order to examine the genetic basis for shape and size covariation between leaves and petals, the allometry model was also used. The petal and leaf modeled data sets obtained above were combined, which allowed overall trends to be identified. To ensure equal weighting of the data from different organs, the organ size for all plants was multiplied by a constant factor so that the variance in the Leaf4, Leaf7, and petal data sets was equal. The Leaf4, Leaf7, and petal data sets were then combined to create a Leaf4-Petal and Leaf7-Petal data sets containing each plant from the MAGIC line groups. Additionally, a PCA was applied to the Leaf4-Petal and Leaf7-Petal data sets to detect correlated variation in the positions of points and to identify trends in shape and size variation between the two organs.

In the Leaf4-Petal model, the PC1 accounted for 53.58% of the total variance representing the negative size covariation between the Leaf4 and petal. The higher the PC1 value, the larger the petal size, and the smaller the fourth leaf size were. The PC2 accounted for 30.26% of the total variance representing the positive size covariation between the fourth leaf and petal. The higher the PC2 value, the larger the petal and leaf size were. The PC3 accounted for 5.92% of the total variance representing the positive shape (mainly in width) covariation between the fourth leaf and the petal. The higher the PC3 value, the more rounded the leaves and petal, and the shorter the petiole was. The PC4 accounted for 3.23% of the total variance representing the negative shape (mainly in width) covariation between the fourth leaf and the petal. The higher the value, the narrower the leaves, the longer the petiole, and the more rounded the petals were. The other PCs represented only one organ shape or size variance, so they were not considered for further analysis (Figure 3).

After QTL mapping in the MAGIC lines for the Leaf4-Petal model, three significant QTLs for PC1, one significant QTL for PC2, two significant QTLs for PC3, and six significant QTLs for PC4 were identified (Figure 5, Supplementary Table 5, Supplementary Figure 7). In each QTL, the candidate genes containing nonsynonymous SNPs unique to the maximal effects accession in the 95% confidence region were identified (Supplementary Table 6 and 7). In PC1, there were five genes with the unique maximal effects accession allele, including the cell-proliferation-related genes, such as *ARGOS*, *LOM2*, and *EXPB5*. In PC3, which represented the shape (mainly in width) covariation, four genes were identified: *ARGOS*, *FRS3*, *BSL3*, and *extensin proline-rich1*. In PC4, representing the negative shape (mainly in width) covariation, there were also four genes containing the unique accession allele. Among these genes, the *CYCD2;1* gene acting on the G1 phase of the cell cycle to control cell division rate in both the shoot and root meristems had an allele unique to the *Hi-0* accession, and the *PRX53* gene influencing cell elongation had an allele unique to the *Po-0* accession.

Similar to the Leaf4-Petal model, in the Leaf7-Petal model, the PC1 accounted for 68.58% of the total variance, representing the negative size covariation between the seventh leaf and petal, whereas the PC2 accounted for 22.51% of the total variance, representing the positive size covariation between the seventh leaf and the petal and also the seventh leaf shape variance. The PC3 accounted for 2.84% of the total variance, representing the positive shape (mainly in width) covariation, and the PC4 accounted for 1.99% of the total variance, representing the negative shape (mainly in width) covariation. The other PCs represented only one organ shape or size variance, so they were not considered for further analysis (Figure 4).

After QTL mapping in the MAGIC lines for the Leaf7-Petal model, two significant QTLs for PC3 and six significant QTLs for PC4 were identified, whereas no significant QTL was identified in PC1 and PC2 (Figure 5, Supplementary Table 5, Supplementary Figure 8). Moreover, the candidate genes were also identified (Supplementary Table 6 and 7). The QTL LF7PE_3.2 in PC3, which represented the positive shape (mainly in width) covariation between the seventh leaf and petal, had the most rounded leaf and petal in *Ler-0* and the narrowest leaf and petal in *No-0* accession. In the 95% confidence region, there were 34 genes conferring alleles unique to the *Ler-0* or *No-0* accession. Among these genes, GRF gene *AT2G22840*, pentatricopeptide repeat protein SLOW GROWTH1 (SLO1), ORGAN BOUNDARY1 (OBO1) and OVATE family of protein OFP16 had been reported affected the organ shape or size (Kim et al., 2003; Sung et al., 2010; Cho et al., 2011; Wang et al., 2011). Furthermore, the cyclin-dependent kinase inhibitor KRP4 (Schiessl et al., 2014) and the serine/threonine-protein kinase PINOID (PID) were involved in the regulation of auxin signaling (Saini et al., 2017). *Growth-regulating factor 3* (*GRF3*), which regulates cell expansion in leaves and cotyledons tissues (Kim et al., 2003), as well as other genes associated with cell differentiation, cell expansion, cell wall modification, and flower time control genes, were also identified. The QTL LF7PE_4.4 in PC4, which represented the negative shape (mainly in width) covariation, had the narrowest leaves with the longest petiole and the most rounded petals in the *Po-0* accession. There were three genes with an allele unique to the *Po-0* accession, including *DME*, a transcriptional activator involved in gene imprinting; *Peroxidase 2*, which influences cell elongation (Jin et al., 2011) and *CYP712A2*, a member of CYP712A.

Discussion

In this study, we defined a genetically controlled allometric space that captured most of the variation in leaf and petal shape and size among MAGIC lines. Among the loci identified, with the exception of the ER locus, the other QTLs were not identical to previously identified shape- and size-associated loci. Additionally, in these QTL confidence regions, many cell-proliferation and cell-expansion-associated genes were isolated with a unique allele according to the accession distribution. Furthermore, we also checked the candidate genes expression data and compared their promoter sequences in the 19 founder accessions of MAGIC lines, and found two candidate genes *ERECTA* (*AT2G26330*) and *AGO4* (*AT2G27040*) in the ER locus on chromosome 2 had specific variation in promoter sequences unique to the maximal effects of accession. Besides, the specific promoter sequence variation also changed the

expression level significantly (Supplementary Figure 11). However, more work is needed to test these loci, such as by constructing a NIL population.

The interaction of leaf and petal shape and size variation

Interestingly, when we augmented the leaves and petal data to investigate the leaf and petal allometry covariation, the results showed that negatively correlated changes in leaf and petal size provided the largest component of allometric variation among MAGIC lines. The QTLs on chromosome 3 for Leaf4-Petal.PC1 overlapped with QTLs for Leaf4.PC1 with the smallest leaf size and the largest petal size in the *Can-0* accession allele. This indicated that the locus positive regulating the fourth leaf size also negatively regulated the petal size. The QTL on chromosome 2 for Leaf4-Petal.PC3 overlapped with Leaf4.PC2 and Petal.PC2 with the widest leaf and petal in the *Ler-0* accession allele, which indicated that the locus positively regulated both the leaf and petal width. The QTL on chromosome 2 for Leaf4-Petal.PC4 was identical to the QTL for Petal.PC2 with the same accession allele effects distribution. Moreover, the QTL on chromosome 5 was identical to the QTL for Petal.PC2 with uncorrelated allele effects distribution. In Leaf7-Petal.PC4, the QTL on chromosome 2 was identical to the QTL for Leaf7.PC2 and overlapped with the ER locus for Petal.PC2 with the maximum allele effects in *Ler-0* accession. Two QTLs on chromosome 5 for Leaf7-Petal.PC4 overlapped with the QTL for Petal.PC2, and the overlapped QTLs LF7PE_4.6 and PE_2.9 both obtained the minimum values in *Ws-2* accession. Besides these overlapped QTLs with leaf or petal allometry, others did not overlap and may have been the independent locus for leaf and petal covariation.

The leaf and petal allometry coordinated with local adaption

Additionally, life-history traits, such as days to bolting, days to flower, rosette leaf number, branch number, and stem height, were also measured in the MAGIC lines. Although many significant phenotype correlations were found (Figure 2), there were overlapping QTLs that could be used to explain the genetic correlation that was identified. After QTL mapping for these life-history traits (Figure 5, Supplementary Table 8 and 9, Supplementary Figure 9), the QTLs for the life-history traits and for the leaf and petal allometry model were compared (Supplementary Figure 10). In Leaf4.PC1, the QTL LF4_1.1 overlapped with one linked QTL - RN.6, for rosette leaf number, and showed the same allele distribution with maximum values in *Po-0* accession. In Leaf7.PC2, the QTL LF7_2.1 on chromosome 2 (~11.2 Mb) overlapped with three linked QTLs (DF.4, DF.5, and DF.6) for days to flower, with the highest value found in the *Bur-0* accession allele. In Petal.PC1, two QTLs, PE_1.2 on chromosome 1 (~16.9 Mb) and PE_1.3 on chromosome 4 (~0.05 Mb), overlapped with the QTLs RN.1 and RN.9 separately for rosette leaf number with uncorrelated allele distribution. In Petal.PC2, there were four QTLs overlapping with the QTLs for days to bolting. Among these QTLs, the QTLs PE_2.2 and PE_2.3 on chromosome 1 overlapped with the QTL DB.1, with the maximum value in the *Po-0* allele. Moreover, PE_2.9 on chromosome 5 overlapped with DB.6, with a maximum value in *Can-0* accession. Others showed uncorrelated allele distribution. There were also four QTLs for Petal.PC2 that overlapped with the QTLs for days to flower, and all showed uncorrelated allele distribution. The overlapped QTL for leaf and petal allometry with life-history traits

provided a genetic basis in correlation analysis. This co-localization may have resulted from pleiotropy or tightly linked causal genes, which indicated genetic integration among all traits.

The advantage of using an allometry model was that the effect of each leaf and petal shape and size variation could be fully described quantitatively with a vector, and the allometric spaces could be captured based on PCs. Conversely, the model was restricted to 2D morphological traits and could neither capture 3D effects, such as curvature changes nor capture the special shape of a leaf, such as a simple leaf with serrations. Besides that, we only explored one environmental condition. Many environmental factors, such as abiotic stress, could have had an effect on leaf and petal shape and size. Analysis of MAGIC lines grown under different conditions could be an additional application of the method.

Conclusions

This is the first report on the genetic basis of allometry variation of leaf and petal and their interaction under the incorporated framework by using the MAGIC lines. PCA for the MAGIC lines indicated that size variation was a major component of allometry variation and revealed negatively correlated changes in leaf and petal size. In this study, five QTLs for the fourth leaf, 11 QTLs for the seventh leaf, and 12 QTLs for the petal size and shape were identified. These QTLs were not identical to those previously identified, with the exception of the ER locus. This indicated that the allometry variation was not simply the combination of organ width, length, and size. Besides, after QTL analyzing the leaf and petal integrated model, 12 QTLs were identified in association with the fourth leaf and petal allometry covariation, and eight QTLs were identified to associate with the seventh leaf and petal allometry covariation. The QTL overlap explained the allometry correlation within different leaves and also the homologous organs-leaf and petal. However, some specific QTLs exited between leaf4 and leaf7 may explain the leaf allometry divergence, which may associated with leaf developmental constrains. Additionally, the correlation of life history traits with leaf and petal allometry and the QTL overlap hinted at the genetic integration and the interaction of organ allometry with local adaptation.

Methods

Plant material and growth conditions

The large population of 527 RILs (Kover et al., 2009) was obtained from University of Oxford, in United Kingdom, and then propagated at Shandong Normal University, in China. Seeds were sterilized for 10 minutes in 75% ethanol, washed in 95% ethanol four to six times, and then suspended in 0.1% agar. All lines were grown separately in a 1/2 Murashige and Skoog medium. The seeds were subsequently grown under the following conditions in a plant incubator (Percival Scientific, Inc): 22°C /18°C (Day/Night) and a long photoperiod of 16 hours/8 hours (Day/Night) after the treatment for four days at 4°C in the dark for stratification. After they were grown in the medium for seven days, the seedlings were transplanted into soil when the true leaves could be seen. For each line, we planted eight seedlings, with four seedlings to

each pot, which was randomly assigned to a tray. The trays were rotated throughout the incubator every week.

Leaf and petal collection

After the first flower of the plant had opened, the fourth and seventh leaves of each plant were picked, flattened, and then glued onto paper to scan in order to record the leaf's shape. Totally, the fourth leaves were obtained from 232 lines and the seventh leaves were obtained from 215 lines (Supplementary Table 1). Because the leaves are more susceptible to environmental influences during growth, we calculated the average area of all obtained leaves in the same line and retained leaves with a difference in the range of +/- 20% for further analysis. To measure the shape of the petals, we picked and dissected the floral buds using a stereomicroscope at fully reflexed petal stage 13 when the buds had fully opened and the petals were visible and in anthesis. All four petals, four sepals, six stamens, and one pistil were removed, placed on 1% agar on a plate, and photographed with a Leica camera. Only buds between bud positions 4 and 10 on the main stem were used. Two flowers were dissected per plant, and each line we collected had at least four plants. Since some of these lines did not bloom properly under current planting conditions, we finally obtained petals from 345 lines for model construction. (Supplementary Table 1).

Modeling in leaves and petals

To generate a parameterized space that captured variation in leaf and petal shape and size, the outlined organs were obtained for intercrossing populations of *Arabidopsis* derived from MAGIC lines. To investigate the allometric variation in the *Arabidopsis* leaf and petal, plants were grown together in a glasshouse, and their fully expanded leaves and petals were flattened and imaged. For each independent line, digital images were taken from 8 independent, mature (after the first flower flowered) fourth and seventh true leaves. A digital image was made of a flattened leaf taken from the fourth and seventh nodes from the base of each plant, and 25 points were placed around the leaf outline using the leaf (Le) template. The resulting leaf shapes were aligned through translation and rotation (Procrustes alignment, Goodall, 1991) to generate a data set in which the outline of a leaf was represented by the Cartesian coordinates of its 25 points, each expressed in standard deviation from the mean position of the point within the collection of leaves. An equivalent procedure was used to generate a petal data set using a 25-point petal (Pe) template.

After all the lines of the fourth and seventh leaves and the petals were prepared, the leaves were properly oriented (with the tip always pointing to the right, and good horizontality) using Photoshop software (Adobe). We used MATLAB (MathWorks) and the AAM Toolbox (Bensmihen et al., 2008) to construct the model of each individual leaf and petal separately. After placing the landmarks, the secondary landmark points were evenly spread along the leaf outline. This was achieved by taking two primary points and fitting a spline between them using the secondary points; a spline being a special function that was defined piecewise by polynomials. The secondary points were then rearranged to be equidistant from each other along the spline. Models including the fourth leaf (Leaf4), the seventh leaf (Leaf7), and petals were separately generated using the AAM Toolbox (version 6.5). Points placed around each leaf and petal

outline were plotted to show the pattern of allometry in the data set. Because the positions of the outline points were unlikely to change independently of one another, a PCA was used on the whole data set to identify trends in variation.

Statistical analyses

Broad sense heritability (H^2) for each trait was estimated as the ratio of the variance among lines to the total variance. To determine phenotype correlations between traits, pairwise Pearson correlations between the line means were calculated. QTL analyses were then performed using the R software package HAPPY as described by Kover et al. (2009). Briefly, this approach used a hidden Markov model to make a multipoint probabilistic reconstruction of the genome of each MAGIC line as a mosaic of the founder haplotypes. Thus, at each marker, a probability of being derived from each of the parental accessions was assigned to each line, and our hypothesis that there would be no QTL was evaluated by fitting a fixed-effect linear model with up to 18 degrees of freedom. We performed QTL analysis for the line average of the Leaf4, the Leaf7, the petal PCs, the argument of the Leaf4-Petal PCs, the argument of the Leaf7-Petal PCs, and the life-history traits. Two QTLs located less than 1 Mb apart were considered overlapping QTLs reflecting the genetic pleiotropy (Gnan et al., 2014).

Abbreviations

MAGIC: Multiparent advanced generation intercross

PCA: Principal component analysis

PCs: Principal components

QTL: Quantitative trait loci

Declarations

Ethics approval and consent to participate

Not applicable

Consent for publication

Not applicable

Availability of data and materials

The raw data used for this research and the supplementary material are available in the Figshare (https://figshare.com/s/90c637df9f8965f346c8). The Dataset 1, which is used for PCA, contains all the cropped images and point models for each plant in MAGIC lines. Meanwhile, the values of each PC and the life history traits for each plant in MAGIC lines are listed in the Dataset 2. The Dataset 3 is the record

of correspondence between planting ID and the MAGIC line ID. The File 1 contains the R source code files for QTL mapping in MAGIC lines.

Competing interests

The authors declare that they have no competing interests.

Funding

This work was support by programs from the National Natural Science Foundation of China (under grant nos. 31470286 and 31801387). The funding organizations played no role in the design of study and collection, analysis, and interpretation of data and in writing the manuscript.

Authors' contributions

SXY and XZF conceived the project and designed this work. XL, CXW and QS performed experiments, YHZ and XL analyzed data. SXY and XZF wrote the manuscript.

Acknowledgements

We are very grateful to Professor Enrico Coen of the John Innes Center for supplying seeds of the 527 MAGIC lines. We also thank LetPub (www.letpub.com) for its linguistic assistance during the preparation of this manuscript.

References

Abraham MC, Metheetrairut C, Irish VF. Natural variation identifies multiple loci controlling petal shape and size in *Arabidopsis thaliana*. PLoS One. 2013; 8:e56743.

Alonso-Blanco C, Koornneef M. Naturally occurring variation in *Arabidopsis*: an underexploited resource for plant genetics. Trends Plant Sci. 2000; 5:22–29.

Anastasiou E, Lenhard M. Growing up to one's standard. Curr Opin Plant Biol. 2007; 10:63–69.

Bensmihen S, Hanna AI, Langlade NB, Micol JL, Bangham A, Coen ES. Mutational spaces for leaf shape and size. HFSP J. 2008; 2:110-120.

Cho E, Zambryski PC. ORGAN BOUNDARY1 defines a gene expressed at the junction between the shoot apical meristem and lateral organs. Proc Natl Acad Sci U S A. 2011; 108:2154-2159.

Costa MM, Yang S, Critchley J, Feng X, Wilson Y, Langlade N, Copsey L, Hudson A. The genetic basis for natural variation in heteroblasty in *Antirrhinum*. New Phytol. 2012; 196:1251-1259.

Czesnick H, Lenhard M. Size control in plants–lessons from leaves and flowers. Cold Spring Harb Perspect Biol. 2015; 7: a019190.

Davila Olivas NH, Frago E, Thoen MPM, Kloth KJ, Becker FFM, van Loon JJA, Gort G, Keurentjes, JJB, van Heerwaarden J, Dicke M. Natural variation in life history strategy of *Arabidopsis thaliana* determines stress responses to drought and insects of different feeding guilds.Mol Ecol. 2017; 26:2959-2977.

E. Powell A, Lenhard M. Control of organ size in Plants.Curr Biol. 2012; 22:360–367.

Feng X, Wilson Y, Bowers J, Kennaway R, Bangham A, Coen E, Hudson A. Evolution of allometry in antirrhinum. Plant Cell. 2009; 21:2999-3007.

Galen C. Solar furnaces or swamp coolers: costs and benefits of water use by solar-tracking flowers of the alpine snow buttercup, Ranunculus adoneus. Oecologia. 2006; 148, 195–201.

Gan X, Stegle O, Behr J, Steffen JG, Drewe P, Hildebrand KL, Lyngsoe R, Schultheiss SJ, Osborne EJ, Sreedharan VT, Kahles A, Bohnert R, Jean G, Derwent P, Kersey P, Belfield EJ, Harberd NP, Kemen E, Toomajian C, Kover PX, Clark RM, Rätsch G, Mott R. Multiple reference genomes and transcriptomes for *Arabidopsis thaliana*. Nature. 2011; 477:419-423.

Gnan S, Priest A, Kover PX. The genetic basis of natural variation in seed size and seed number and their trade-off using *Arabidopsis thaliana* MAGIC lines. Genetics. 2014; 198:1751-1758.

Goodall C. Procrustes methods in the statistical analysis of shape. J R Stat Soc B. 1991; 53:285-339.

Jin J, Hewezi T, Baum TJ. *Arabidopsis* peroxidase AtPRX53 influences cell elongation and susceptibility to Heterodera schachtii. Plant Signal Behav. 2011; 6:1778-1786.

Juenger T, Perez-Perez JM, Bernal S, Micol JL. Quantitative trait loci mapping of floral and leaf morphology traits in *Arabidopsis thaliana*: evidence for modular genetic architecture. Evol Dev. 2005; 7:259–271.

Kaplan-Levy RN, Quon T, O'Brien M, Sappl PG, Smyth DR. Functional domains of the PETAL LOSS protein, a trihelix transcription factor that represses regional growth in *Arabidopsis thaliana*.Plant J. 2014; 79:477-491.

Kim JH, Choi D, Kende H. The AtGRF family of putative transcription factors is involved in leaf and cotyledon growth in *Arabidopsis*. Plant J. 2003; 36:94-104.

Klingenberg CP. Quantitative genetics of geometric shape: Heritability and the pitfalls of the univariate approach. Evolution. 2003; 57:191–195.

Klingenberg CP. Size, shape, and form: concepts of allometry in geometric morphometrics. Dev Genes Evol. 2016; 226:113-137.

Kover PX, Valdar W, Trakalo J, Scarcelli N, Ehrenreich IM, Purugganan MD, Durrant C, Mott R. A Multiparent Advanced Generation Inter-Cross to fine-map quantitative traits in *Arabidopsis thaliana*. PLoS

Genet. 2009; 5:e1000551.

Langlade NB, Feng X, Dransfield T, Copsey L, Hanna AI, Thébaud C, Bangham A, Hudson A, Coen E. Evolution through genetically controlled allometry space. Proc Natl Acad Sci U S A. 2005; 102:10221-10226.

Li Y, Cheng R, Spokas KA, Palmer AA, Borevitz JO. Genetic variation for life history sensitivity to seasonal warming in *Arabidopsis thaliana*. Genetics. 2014; 196:569-577.

Maugarny-Calès A, Laufs P. Getting leaves into shape: a molecular, cellular, environmental and evolutionary view. Development. 2018; 145:dev161646.

McDonald PG, Fonseca CR, Overton JM, Westoby M. Leaf-size divergence along rainfall and soil-nutrient gradients: is the method of size reduction common among clades? Func Ecol. 2003; 17:50–57.

Moyroud E, Glover BJ. The evolution of diverse floral morphologies.Curr Biol. 2017; 27:941-951.

Pérez-Pérez JM, Serrano-Cartagena J, Micol JL. Genetic analysis of natural variations in the architecture of *Arabidopsis thaliana* vegetative leaves. Genetics. 2002; 162:893-915.

Prpic NM, Posnien N. Size and shape-integration of morphometrics, mathematical modelling, developmental and evolutionary biology. Dev Genes Evol. 2016; 226:109-112.

Saini K, Markakis MN, Zdanio M, Balcerowicz DM, Beeckman T, De Veylder L, Prinsen E, Beemster GTS, Vissenberg K. Alteration in auxin homeostasis and signaling by overexpression of PINOID kinase causes leaf growth defects in *Arabidopsis thaliana*. Front Plant Sci. 2017; 8:1009.

Schiessl K, Muiño JM, Sablowski R. *Arabidopsis* JAGGED links floral organ patterning to tissue growth by repressing Kip-related cell cycle inhibitors. Proc Natl Acad Sci U S A. 2014; 111:2830-2835.

Smith J, Burian R, Kauffman S, Alberch P, Campbell J, Goodwin B, Lande R, Raup D, Wolpert L. Developmental constraints and evolution: A perspective from a mountain lake. Q Rev Biol. 2014; 60:265–286.

Sung TY, Tseng CC, Hsieh MH. The SLO1 PPR protein is required for RNA editing at multiple sites with similar upstream sequences in *Arabidopsis* mitochondria. Plant J. 2010; 63:499-511.

Wang S, Chang Y, Guo J, Zeng Q, Ellis BE, Chen JG. *Arabidopsis* ovate family proteins, a novel transcriptional repressor family, control multiple aspects of plant growth and development. PLoS One. 2011; 6:e23896.

Weigel D. Natural variation in *Arabidopsis*: from molecular genetics to ecological genomics. Plant Physiol. 2012; 158:2-22.

Supplementary Material

Additional file 1: Figure S1-S11.

Figure S1. PCA was applied to the Leaf4, Leaf7, and petal data set to identify trends in shape and size variations among MAGIC lines.

Figure S2. Range of PC values obtained for leaf and petal allometric model.

Figure S3. Variation along each PC for Leaf4, Leaf7 and Petal allometry within the MAGIC lines.

Figure S4-S6. QTL scan of the PCAs for the fourth leaves, seventh leaves and petals allometry among MAGIC lines.

Figure S7-S8. QTL scan of the PCAs for the fourth leaves and petals allometry covariation among MAGIC lines.

Figure S9. QTL scan of the life-history traits among MAGIC lines.

Figure S10. The genetic correlation between life-history traits and allometry model.

Figure S11. The promoter sequence alignment and expression analysis of candidate genes.

Additional file 2: Table S1. The phenotype data for all traits used for QTL analysis.

Additional file 3: Table S2. Significant QTL detected for the leaf and petal allometry models.

Additional file 4: Table S3. The estimated value for each of the 19 parental alleles at each detected QTL for leaf and petal allometry models.

Additional file 5: Table S4. The candidate genes account for leaf and petal allometry variation.

Additional file 6: Table S5. Significant QTL detected for the leaf and petal allometry covariation.

Additional file 7: Table S6.The estimated value for each of the 19 parental alleles at each detected QTL for leaf and petal allometry covariation.

Additional file 8: Table S7. The candidate genes account for leaf and petal allometry covariation.

Additional file 9: Table S8. The significant QTL detected for life-history traits in MAGIC lines.

Additional file 10: Table S9. The estimated value for each of the 19 parental alleles at each detected QTL for life-history traits.

Tables

Table 1. Phenotypic variation among MAGIC lines for leaf and petal allometry models

Trait	Min	Max	Mean ± SD	H^2
Leaf4.PC1	-103.05	101.52	1.68 ± 31.9	0.83
Leaf4.PC2	-39.84	42.86	-0.22 ± 13.4	0.67
Leaf7.PC1	-226.53	270.35	-2.54E-09 ± 70.0	0.87
Leaf7.PC2	-81.51	68.12	1.08E-08 ± 26.4	0.77
Leaf7.PC3	-47.81	72.20	2.95E-09 ± 14.7	0.62
Petal.PC1	-86.65	56.59	0.01 ± 24.1	0.83
Petal.PC2	-20.83	30.18	-0.001 ± 6.7	0.74

Minimum (Min), maximum (Max) phenotypic values for each trait, as well as the phenotypic mean plus or minus their standard deviation (SD) and their broad-sense heritability (H^2), are shown.

Figures

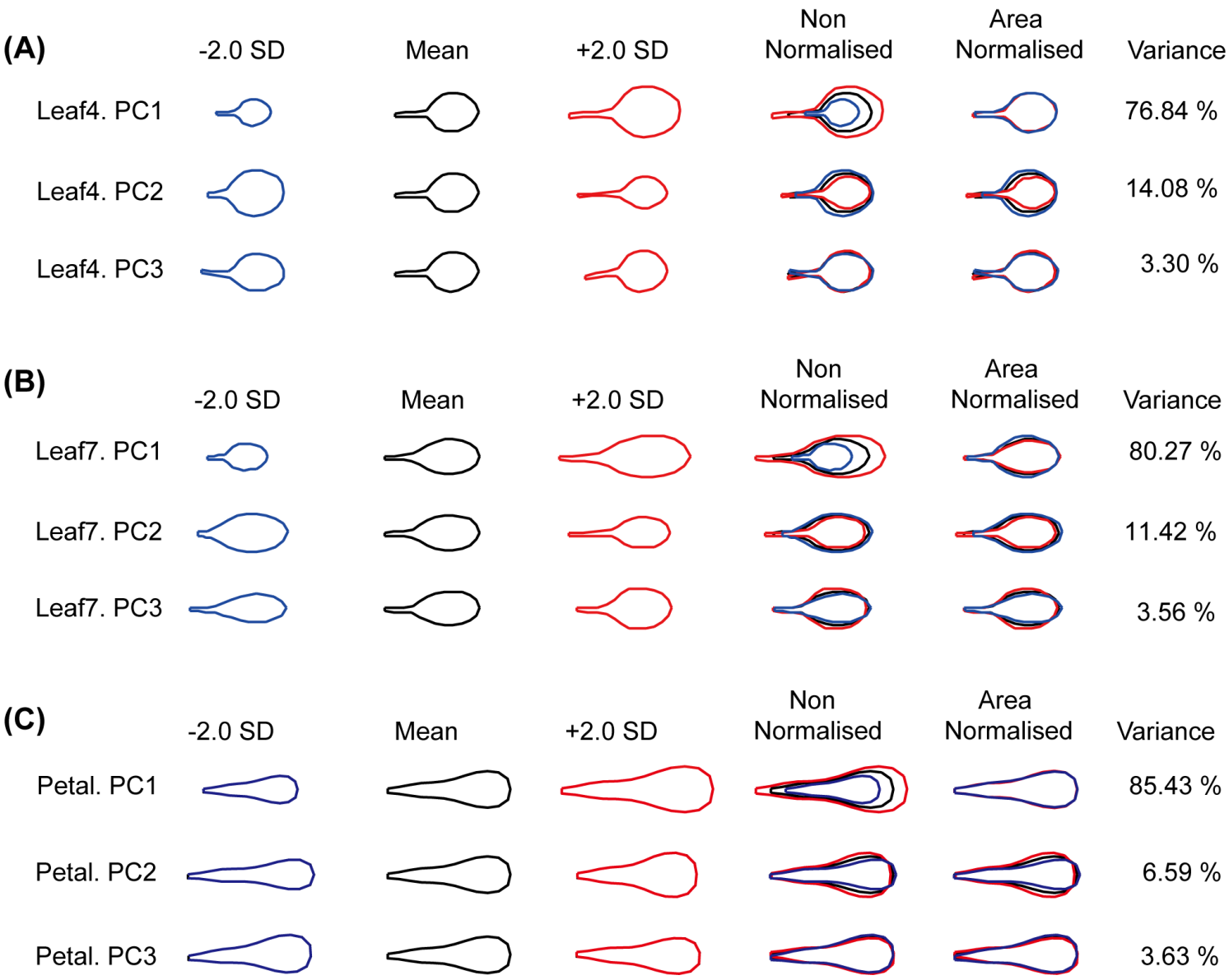

Figure 1

Leaf and petal allometry models for multiparent advanced generation intercross (MAGIC) lines. Allometry models describe variations in the shape and size of the leaves (with the fourth and the seventh leaves) and petals in terms of principal components (PCs). The effects on the leaf and petal outlines, corresponding to decreasing or increasing each PC by two standard deviations from the mean for all samples, are shown on the left. The overlaid outlines are shown to the right, after adjusting to the same area (Area Normalized) to illustrate the effects of each PC on organ shape, or without normalization (Non-normalized). The proportion of the total variance in organ shape and size within the group captured by each PC is given as a percentage.

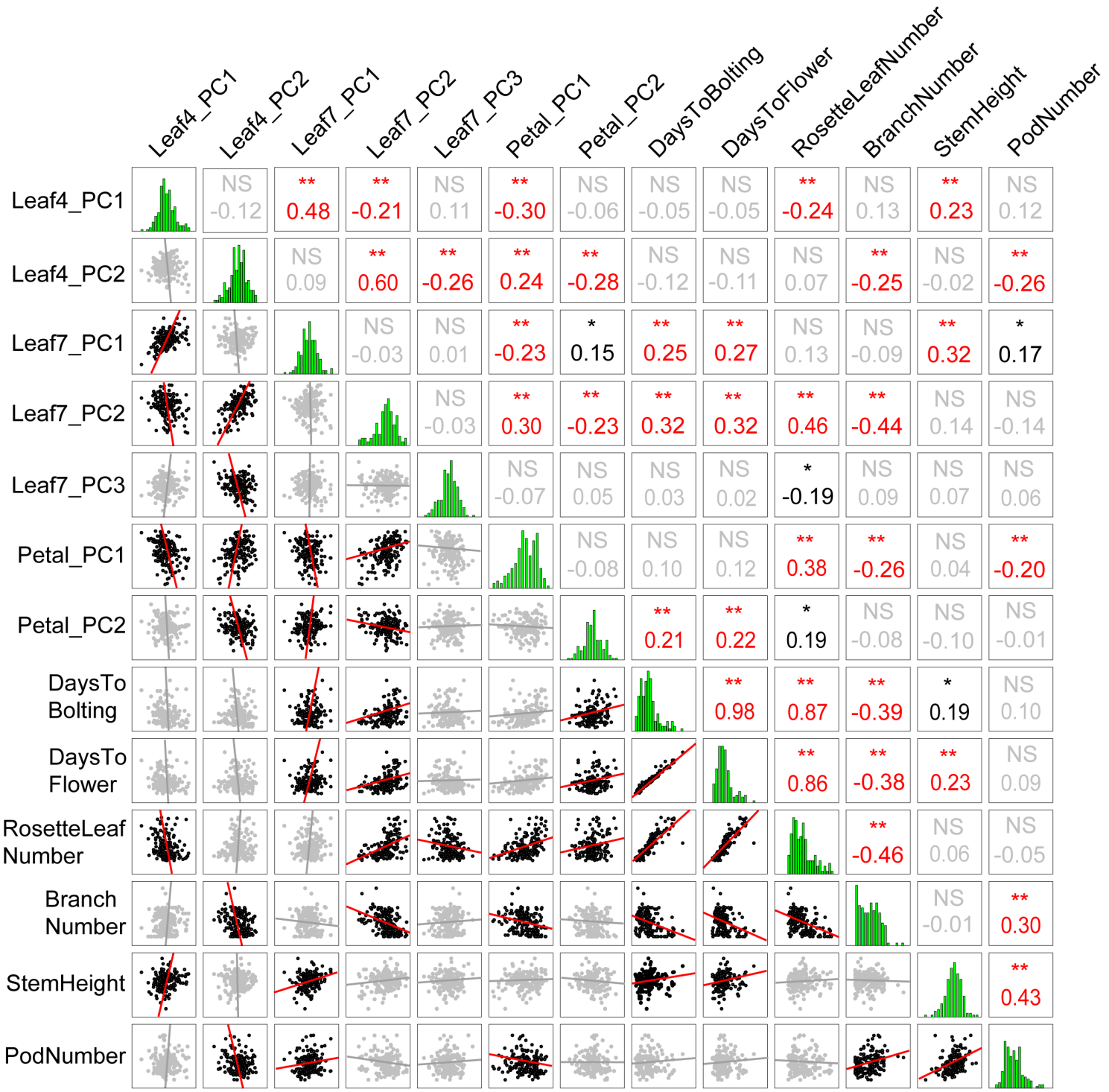

Figure 2

Pairwise Pearson's correlations between the traits measured. All traits measured showed as a normal distribution and Pearson's correlations for leaf and petal allometry, and life history traits in MAGIC lines were performed with significant correlated in red (P < 0.01) and dark (P < 0.05), not significant in grey. NS, not significant; **, correlation is significant at the 0.01 level (two-tailed); *, correlation is significant at the 0.05 level (two-tailed).

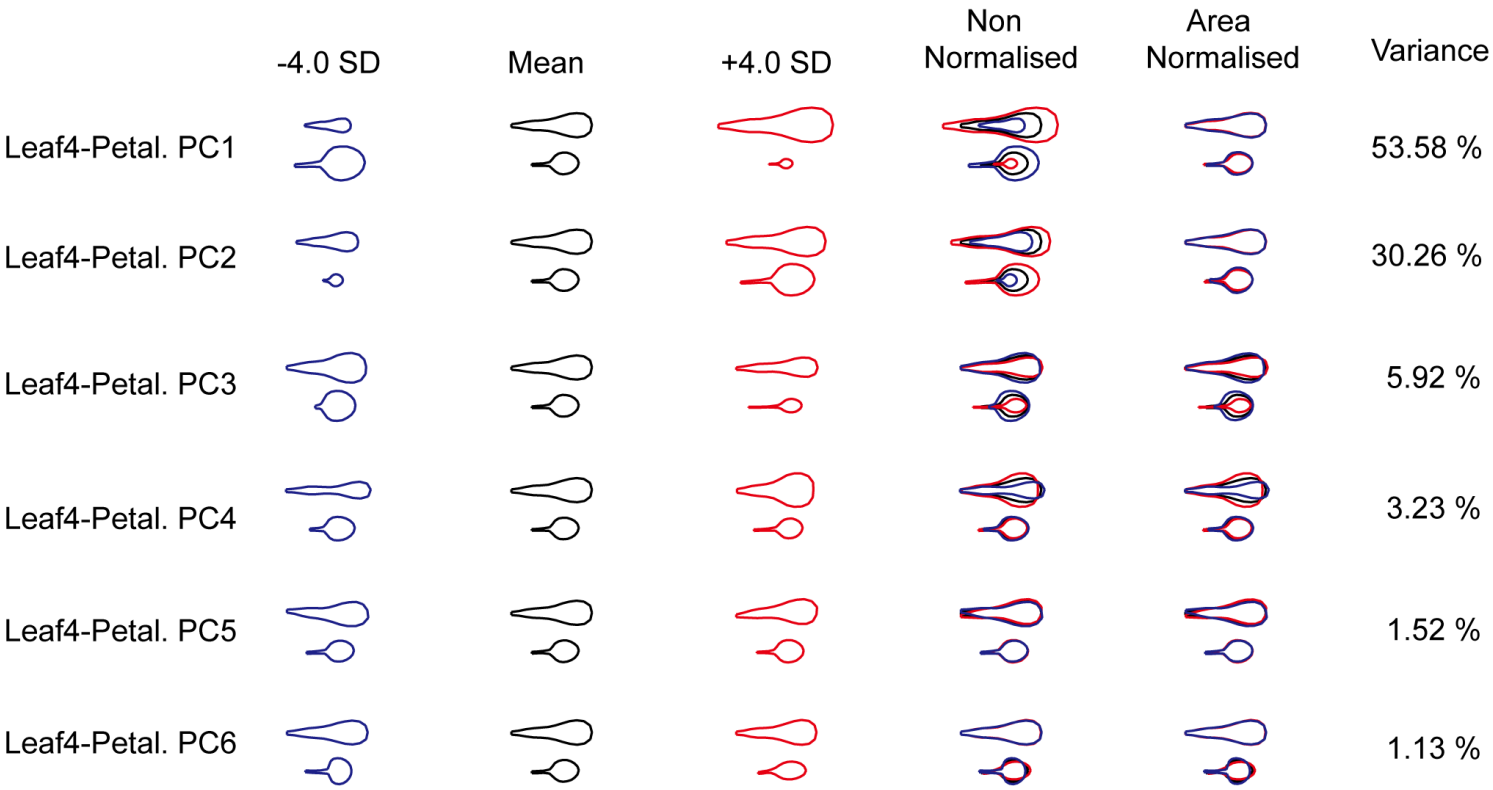

Figure 3

An integrated organ allometry model for the fourth leaves and petals. Covariation in the fourth leaves and petals is described by variation along the first six PCs of a combined leaf and petal allometry model. The effects on the leaf and petal outlines, which corresponded to decreasing or increasing each PC by four standard deviations from the mean for all samples, are shown on the left. Overlaid outlines are shown to the right after adjustment to the same area (Area Normalized) to illustrate the effects of each PC on organ shape, or without normalization (Non-normalized). The proportion of the total variance in organ shape and size within the group that was captured by each PC is given as a percentage.

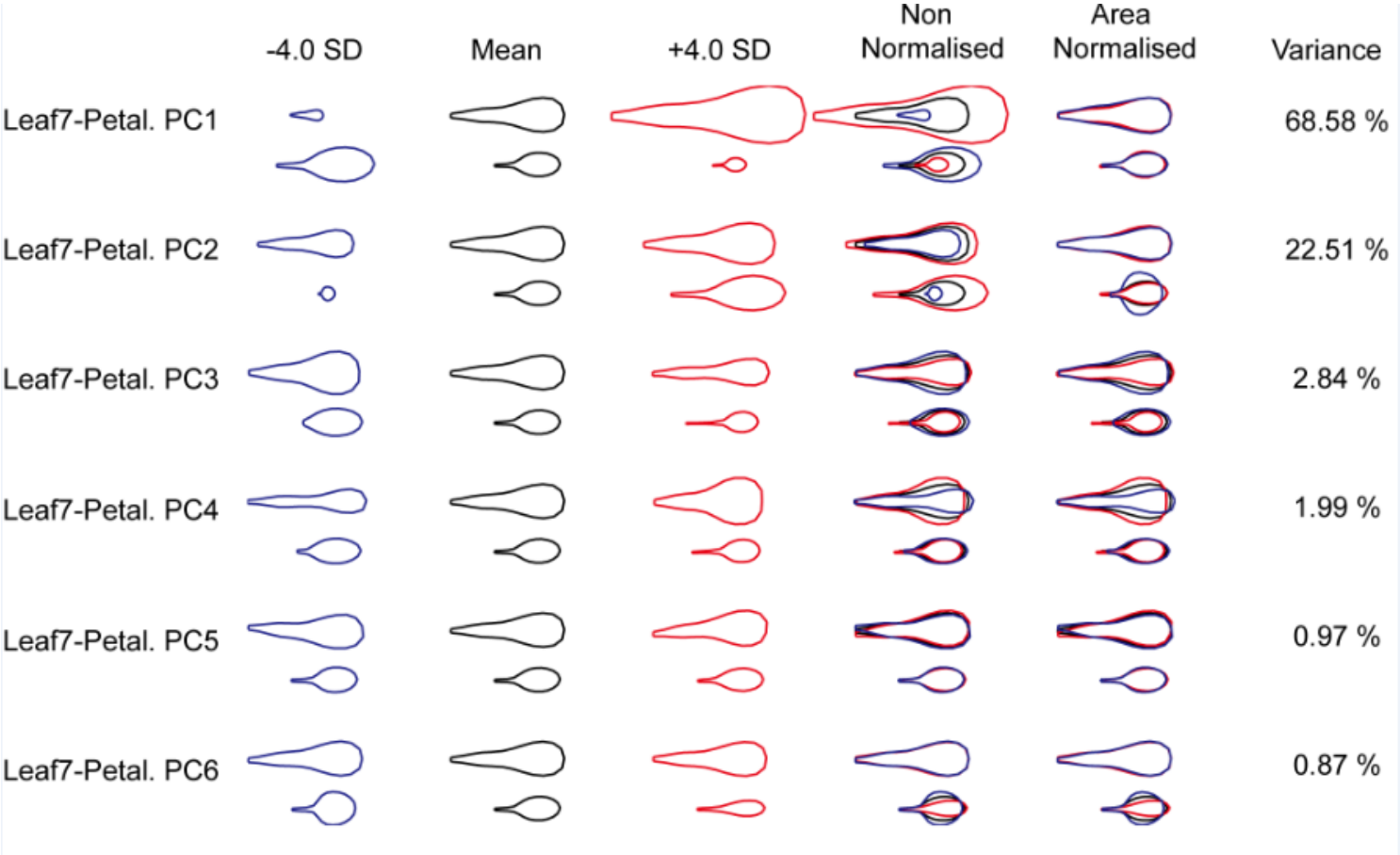

Figure 4

An integrated organ allometry model for the seventh leaves and petals. Covariation in the seventh leaves and petals is described by variation along the first six PCs of a combined leaf and petal allometry model. The effects on the leaf and petal outlines, which corresponded to decreasing or increasing each PC by four standard deviations from the mean for all samples, are shown on the left. Overlaid outlines are shown to the right after adjustment to the same area (Area Normalized) to illustrate the effects of each PC on organ shape or without normalization (Non-normalized). The proportion of the total variance in organ shape and size within the group that was captured by each PC is given as a percentage.

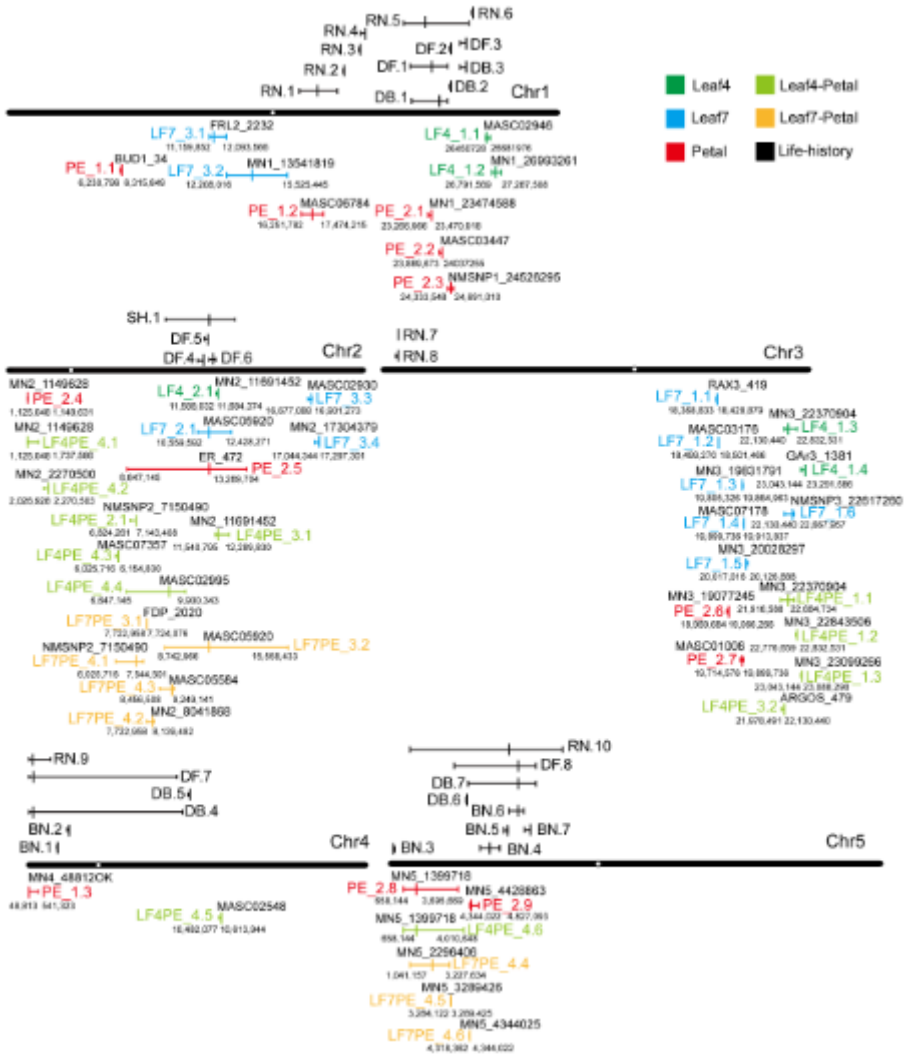

Figure 5

Chromosomal locations of QTL for shape and size variation in Leaf4, Leaf7, petal, Leaf4-Petal, Leaf7-Petal and life history traits in MAGIC lines. The chromosomal location of identified QTLs is shown on the five Arabidopsis chromosomes. Each QTL is indicated by a line segment, with the extent of the line indicating the 95% confidence region and the peak SNP showing by a long vertical line in the QTL region. QTLs for different traits are shown in different colors: the QTLs for Leaf4 allometry showed in dark green and named LF4 (LF4_1, Leaf4.PC1; LF4_2, Leaf4.PC2); the QTLs for Leaf7 allometry showed in blue and named LF7 (LF7_1, Leaf7.PC1; LF7_2, Leaf7.PC2; LF7_3, Leaf7.PC3); the QTLs for petal allometry showed in red and named PE (PE_1, Petal.PC1; PE_2, Petal.PC2); the QTLs for Leaf4-Petal shape and size covariation showed in light green and named L4PE (L4PE_1, Leaf4-Petal.PC1; L4PE_2, Leaf4-Petal.PC2); the QTLs for Leaf7-Petal shape and size covariation showed in orange and named L7PE (L4PE_1, Leaf4-Petal.PC1; L4PE_2, Leaf4-Petal.PC2); the QTLs for life-history traits all showed in dark (BN, Branch Number; DB, Days To Bolting; DF, Days To Flower; RN, Rosette Leaf Number; SH, Stem Height).

Supplementary Files

This is a list of supplementary files associated with this preprint. Click to download.

- Additionalfile2TableS1.xlsx
- Additionalfile3TableS2.xlsx
- Additionalfile4TableS3.xlsx
- Additionalfile5TableS4.xlsx
- Additionalfile6TableS5.xlsx
- Additionalfile7TableS6.xlsx
- Additionalfile8TableS7.xlsx
- Additionalfile9TableS8.xlsx
- Additionalfile10TableS9.xlsx
- Additionalfile1FiguresS1S11.pptx